Chapter 2
Fundamentals of Peptide-Materials Interfaces

Tiffany R. Walsh

Abstract The investigation of the binding, dynamics and properties of peptides adsorbed on inorganic surfaces is an inherently multidisciplinary endeavor. This chapter is primarily aimed at new researchers in this field, to introduce the basic concepts that span physical chemistry, surface science, structural biology, computational techniques, and materials science; all of which are necessary for gaining a comprehensive overview of peptide-materials interfaces. What are the key insights that can be determined from these interfaces? Usually, this will comprise a blend of thermodynamics, kinetics and structural characterizations. Typically, we might wish to compare the binding strength of a peptide, and concomitantly, the structure(s) assumed by the peptide upon adsorption. We might also seek to characterize the surface diffusion, and/or aggregation (or assembly) of these surface-adsorbed biomolecules. These observations serve to facilitate connections between the composition and sequence of the peptide, and its behavior and properties at the interface. Such connections could be subsequently exploited in bioinformatics models to enable the prediction of new peptide sequences, with designed, predictable interfacial properties.

2.1 Introduction and Background

Peptides and proteins are workhorses in the natural world, carrying out a variety of roles, including: recognizers, connectors, transporters, messengers/reporters, and structural support, just to name a few (Whitford 2005). Peptides and proteins are also closely associated with biominerals in Nature, such as in shells, bone, sponge spicules, and tooth enamel (Sarikaya et al. 2003; Crookes-Goodson et al. 2008;

T. R. Walsh (✉)
Institute for Frontier Materials, Deakin University, Geelong, VIC 3216, Australia
e-mail: tiffany.walsh@deakin.edu.au

M. R. Knecht and T. R. Walsh (eds.), *Bio-Inspired Nanotechnology*,
DOI: 10.1007/978-1-4614-9446-1_2,

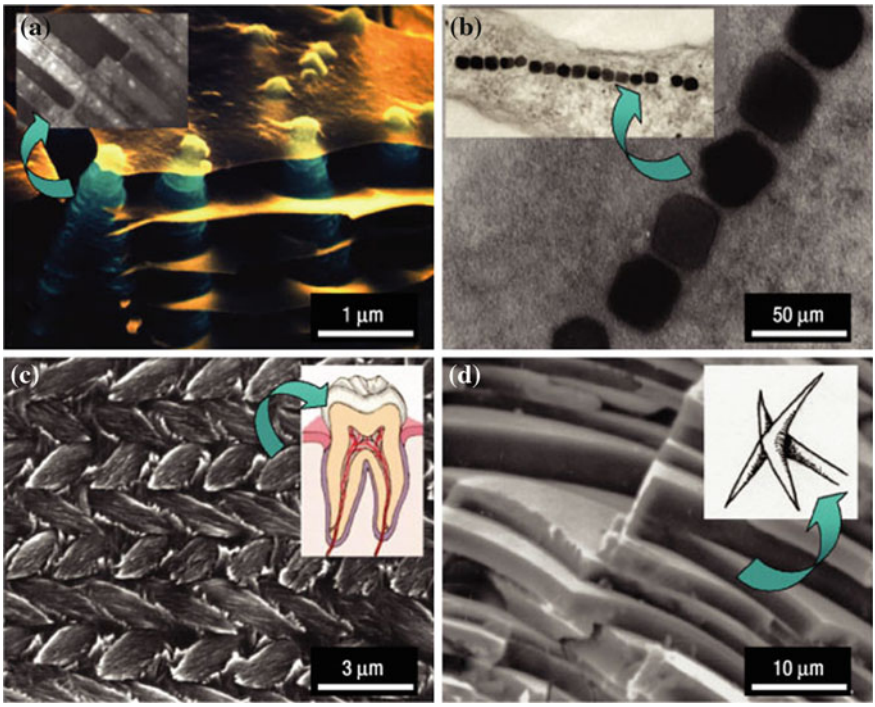

Fig. 2.1 Scanning electron microscopy images of naturally-occurring high-performance bioinorganic composite materials. **a** Aragonite platelets in the growth edge of an abalone shell (*inset* transmission electron microscope, TEM, image); **b** crystallographically-aligned magnetite nanoparticles formed by magnetotactic bacteria (*inset* TEM image); **c** woven nanocrystals of hydroxyapatite in tooth enamel; **d** layered silica of a sponge spicule. Reproduced with permission of the copyright holder, from Sarikaya et al. (2003)

Dickerson et al. 2008a), see Fig. 2.1 for example. Biomineral-associated proteins and peptides are thought to have evolved to play a key role in the nucleation, growth, and organization of nanostructured biocomposite materials. They are thought to do so via specific, noncovalent interactions with the aqueous materials interface. Research in this area spans the investigation of naturally occurring biogenic minerals through to the search and identification of new peptide sequences, associated with artificial hard materials. It is the latter, that of selected peptide sequences that recognize materials through specific noncovalent interfacial interactions, that we will focus on herein in this chapter.

The pioneering work of Stanley Brown, employing cell surface display, first identified peptide sequences that recognized the gold surface (Brown 1997). Since this pioneering work, the research field encompassing the identification and characterization of materials-binding peptide sequences grew rapidly (see, e.g., Whaley et al. 2000; Naik et al. 2002a; Sarikaya et al. 2004); to date these selection data cover peptide sequences identified to bind, for example, metals (Naik et al. 2002b; Forbes et al. 2010; Li et al. 2009; Hnilova et al. 2008; Heinz et al. 2009;

Chiu et al. 2010), oxides (Naik et al. 2002a; Oren et al. 2007; Patwardhan et al. 2012; Sano and Shiba 2003; Dickerson et al. 2008b; Fang et al. 2008; Thai et al. 2004; Nygaard et al. 2002; Rothenstein et al. 2012), semi-conductors (Whaley et al. 2000; Lee et al. 2002; Estephan et al. 2011), nanostructured carbon such as carbon nanotubes and graphite (Kulp et al. 2005; Wang et al. 2003; Cui et al. 2010; Pender et al. 2006), polymers (Serizawa et al. 2007), carbohydrates (Guo et al. 2013), as well as naturally-occurring minerals (Li et al. 2002; Roy et al. 2008, Gungormus et al. 2008). These peptide sequences were typically selected from libraries via an iterative binding process referred to as biopanning (Sarikaya et al. 2003). The final set of selected sequences resulting from the biopanning process are those deemed to confer the strongest ***binding affinity*** (i.e., adsorption strength) for a target material. In addition to these identification studies, peptide sequences have been reported that exhibit a discrimination in terms of surface recognition, sometimes referred to as ***binding selectivity***: discrimination between two (or more) material surfaces (compositional selectivity) (Tamerler et al. 2006; Fang et al. 2008); discrimination between different crystallographic surface orientations of the same material (facet selectivity) (Wright and Walsh 2012; Ruan et al. 2013), and discrimination between two (or more) polymorphs of the same material (polymorph selectivity). Exploitation of this binding selectivity is poised to play a pivotal role in the future adoption of materials-binding peptides into the mainstream deployment of nucleation, growth, and assembly approaches for making novel, synthetic, nanostructured bioinorganic hybrid materials with designed and predictable properties, under ambient conditions.

However, identification of peptide sequences is only the first, albeit crucial, step in the successful utilization of materials-binding selective peptides in realizing this goal. Currently, isolation and identification of materials-binding peptide sequences, per se, do not form the bottleneck in advancing this research field; rather, it is the generation of understanding, and the distillation of *generalizable* principles, derived from this understanding, that at present hinders progress toward these goals. Key unanswered questions remain, and resolution of these questions is central to enabling the incorporation of materials-binding peptides into the toolbox of reliable materials synthesis approaches that can be realized for a variety of different inorganic components, and furthermore, enable the *versatile* creation of novel, multimaterials nanostructured assemblies.

Some of these questions are concerned with experimental approaches, ranging from the fundamental conditions for biopanning and the impact of this on the selected sequences (Puddu and Perry 2012) through to how to directly determine the adsorbed peptide structure(s) at the interface (Mirau et al. 2011). However, one of the more imperative questions in this research topic is associated with interpretation—how can we relate the materials-binding behavior to the peptide sequence (and not just the residue content of the peptide)? This question concerns not only how to interpret outcomes from peptide selection experiments, but also is pivotal to understanding how to systematically preserve the materials-recognition properties of these selected peptides upon conjugation into larger molecular constructs.

2.2 Basic Key Concepts: Surface Science and Physical Chemistry

2.2.1 Introductory Surface and Interface Science

Characterization of the surface of the target material is as important to gaining insight into the adsorption behaviors of materials-binding peptides as the conformations of the peptides themselves. Relevant questions regarding the state of the surface include: is the surface crystalline or amorphous? If crystalline, is the surface single crystal or polycrystalline? What is the charged state of the surface, under aqueous conditions, and at a range of pH values? The process history of the surface samples can be pivotal to understanding the behavior of the surface (particularly for silica) (Patwardhan et al. 2012); is the surface clean—e.g., are there problems with adventitious carbon? If so, is there a way to clean the surface without destroying or modifying the desired surface structure? If the surface is already coated (e.g., with a stabilizing ligand such as citrate, in the case of nanoparticles), how does the presence of the ligand and its distribution on the surface affect peptide binding? Moreover, the shape of the aqueous materials interface could also conceivably play a role in controlling adsorption of peptides, in addition to the consideration of steps and kinks that may be present on planar materials surfaces. For some materials (such as oxides) it can be challenging to separate out the dependencies between surface curvature and surface chemistry for small nanoparticle surfaces (Patwardhan et al. 2012). The propensity of the material surface to oxidize may also create challenges; while some oxide surfaces are well understood from a structural perspective, other materials, e.g., semiconductor surfaces such as GaAs and CdSe, may possess very complex oxide surface structures that are not necessarily well resolved at the atomistic level, thus potentially hindering our understanding of how peptides recognize these materials. Finally, all of these factors regarding the materials surface structure can also play a critical role in determining the structuring of the solvent (usually aqueous solution) at the interface. The impact of this interfacial solvent structuring on the adsorption propensity of materials-binding peptides will be subsequently discussed in more detail (*vide infra*).

Before doing so, we give a brief summary of some common terms and concepts associated with the surface science of crystalline materials. In brief, if a material is crystalline, then the bulk material will feature a regular patterning in three-dimensional (3-D) space in terms of the constituents of the crystal, i.e., the atoms and/or molecules in the material. By cutting the 3-D bulk crystal along a given plane (defined by three noncolinear points in the crystal lattice) different crystalline *surfaces* can be generated, thus presenting different, two-dimensional arrangements of surface atoms—e.g., see Fig 2.2. Types of surfaces are characterized by three numbers known as the Miller indices (*h, k, l*)—e.g., the (111) surface or the (100) surface (as in Fig. 2.2). The vector normal to the Miller Plane is the vector [*h, k, l*]. (see, for example, Atkins and de Paula 2010, for more

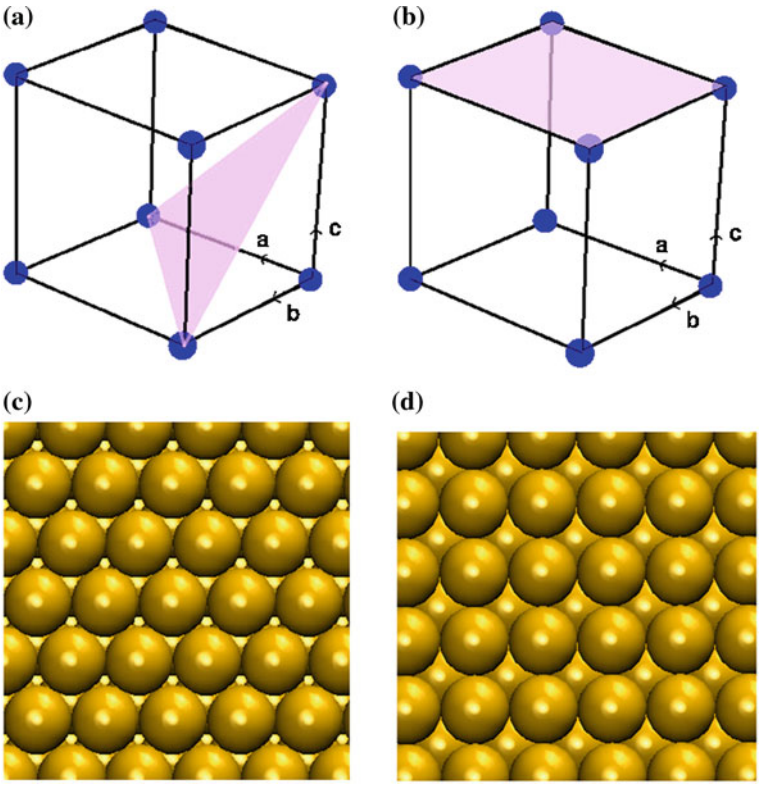

Fig. 2.2 Illustration of different crystallographic orientations of surfaces. **a** and **b** Indicate two lattice planes of a simple cubic lattice, the (111) and (001) planes, respectively. The three principal axes are indicated as $\vec{a}$, $\vec{b}$, and $\vec{c}$. **c** and **d** Give the atomistic-level structure of two different example crystallographic orientations of the ideal gold surface, the (111) and (100) planes, respectively

details). Crystalline surfaces can depart from ideality via the incorporation of defects; e.g., vacancy defects; and through the presence of steps, kinks, and adatoms on the surface. These features may exhibit very different propensities for interaction with adsorbed peptides, compared with the ideal surface. One other point of distinction for crystalline surfaces is the consideration whether the surface is single crystal (e.g., a single crystal Au(111) surface), or, a polycrystalline surface (one that presents an ensemble of different low-energy planes).

A further complication arises in the consideration of crystalline surfaces in terms of surface reconstruction. If we consider cleaving the bulk crystal along a given plane orientation, then the newly generated surface exposes atoms on the surface that are *under-coordinated* in comparison with the atoms underneath the surface layers. This under-coordination may lead to a rearrangement of the surface atoms such that the potential dangling bonds at the surface can be satisfied, a

classic example of which is the (7 × 7) reconstruction of the Si(111) surface (Binnig et al. 1983). While this definition may suggest that covalently bonded network solids are prone to surface reconstruction, it is also possible for other types of materials, e.g., noble metals, to support surface reconstruction. The favorable reconstructions of a surface should be considered, since the subsequent arrangement of the surface atoms could impact substantially on adsorption behavior at the aqueous interface, not only through spatial registry of the collective interactions between the peptide atoms and the surface atoms per se, but also via any changes of the solvent structuring at the reconstructed surface.

Structuring (both spatial and orientational) of interfacial solvent is thought to highly influential on the adsorption structure(s) of the peptide. Part of this influence is possibly due to the changes in the solvent hydrogen-bonded network in the interfacial region, thus perhaps modifying the opportunities for the peptide interact via hydrogen-bonds with this interfacial solvent. In addition, the thermodynamics of peptide adsorption can be influenced by how tightly the solvent is bound to the surface itself, given that the peptide will displace solvent in the first solvation layer if the peptide makes direct surface contact, i.e., non solvent-mediated surface contact (Skelton et al. 2009; Schneider and Colombi-Ciacchi 2012). In free energy terms, there will be a trade-off between the loss of enthalpy of the released first-layer solvent molecules, the gain in enthalpy for the adsorbed peptide groups, the gain in entropy of the interfacial waters released into the bulk—due to the footprint of the parts of the peptide that make direct contact, and thus displace the waters, and the loss in peptide conformational entropy upon adsorption onto the surface. Additional complications arise in the interfacial solvent structuring due to the presence of solvated ions, particularly due to structuring of the electrical double layer for interfacial salt solutions. The influence of salt concentration on the interfacial adsorption of functional groups analogous to peptides has been recently investigated using atomic force microscopy (AFM) (Hassenkam et al. 2012). Finally, the sharpness of the interface between the solvent and the materials surface could potentially exert a significant influence on peptide adsorption; very sharp interfaces (such as for the aqueous noble-metal interface), might show differences in adsorption with the slowly dissolving interface of some materials surfaces (e.g., for silica). However, both of these examples could differ substantially with some carbohydrate surfaces, where ingress of water into the upper surface layers of the material may instead result in a diffuse interfacial layer instead of a sharp interface, thus potentially modulating the binding behaviors of the peptide.

If the target material is amorphous, we cannot know the local arrangement of the atoms on the surface in precise detail. However, we can make statistical inference regarding some average structural characteristics. This is important not only for the bulk material—e.g., in terms of determining the radial distribution function between pairs of atoms in the bulk—but also for the surface structure, such as the average distances between moieties presented on the surface. Average surface densities of relevant groups are also valuable information; e.g., for hydroxylated surfaces, it may be possible to identify the average surface density of hydroxyl groups, as well as the types of hydroxyl (germinal *vs* vicinal) on the surface. Further details

regarding the distribution of these sites, while desirable, are typically not available from experimental data. This creates a challenge for interpreting adsorption data, since many distribution models of the sites can admit the same average site density. The atomistic scale surface topography of the amorphous surface may also be much more rugged compared with an ideal single-crystal surface.

In closing, often one of the most challenging aspects related to surface characterization for materials-binding peptide systems is related to consistency. In other words, is it not uncommon that the target surface against which the peptide library was screened was not, for reasons of practicality, the same surface that was used for subsequent characterization experiments. For example, a peptide may be selected to recognize the quartz(100) surface (crystalline SiO_2), but the peptide-binding characterization may be performed on the amorphous SiO_2 surface. This apparent inconsistency can perhaps be attributed to the common quantitative characterization techniques currently available (quartz crystal microbalance, and, surface plasmon resonance) where the required material surface under study must first be deposited as a thin film on top of the surface of, e.g., the surface plasmon resonance chip. Thin-film deposition of amorphous or polycrystalline materials is viable for a range of materials—deposition of crystalline materials, at present, is not.

2.2.2 Physical Chemistry

Two key viewpoints from which to survey any interfacial process are thermodynamics and kinetics. Thermodynamics is concerned with the state of the system at a given state point (in temperature and pressure) at chemical equilibrium. The reaction kinetics concern the rates at which both peptide adsorption and desorption take place, as well as the rates of interconversion between different peptide conformations in the adsorbed state.

Consider the following chemical equation for peptide adsorption on a surface (Wei and Latour 2008):

$$P + S \rightleftharpoons PS$$

where *P, S* and *PS* represent the peptide in solution, the available surface sites for adsorption, and the peptide in the surface-adsorbed state, respectively. k_{ads} is the forward rate coefficient for the adsorption process, while k_{des} is the reverse rate coefficient for the desorption of the peptide, assuming that the binding process is reversible. The forward and backward rates of reaction can be expressed assuming elementary reaction steps in both instances:

$$\frac{\mathrm{d}[P]}{\mathrm{d}t} = -k_{ads}[P][S]$$

$$\frac{\mathrm{d}[PS]}{\mathrm{d}t} = -k_{\mathrm{des}}[PS].$$

In simplified terms (Pilling and Seakins 2001), the equilibrium constant, K_{ads}, for this reaction can therefore be expressed as:

$$K_{\mathrm{ads}} = \frac{[PS]}{[P][S]}.$$

Equilibrium is dynamic, with both adsorption and desorption taking place, but *at equal rates* such that the concentrations $[PS]$, $[P]$ and $[S]$ are maintained at constant values. This leads to a further expression, relating the ratio of the rate coefficients for both the forwards and backwards reactions to the equilibrium constant:

$$\frac{k_{\mathrm{ads}}}{k_{\mathrm{des}}} = K_{\mathrm{ads}}.$$

At equilibrium, changes in thermodynamic properties (such as the change in free energy), between an initial state and a final state, depend only on the differences in these properties at these state points, and are independent of the pathway taken to proceed from the initial state to the final state (Atkins and de Paula 2010). The key thermodynamic quantity of interest is the change in free energy upon adsorption, although associated quantities, such as the fractional surface coverage are also often reported in adsorption studies. The change in Gibbs free energy corresponding to adsorption of the peptide, ΔG_{ads}, is measured to be the change in free energy at constant temperature and pressure, for an initial state where the peptide is located far from the interface, in bulk solution, and for a final state where the peptide is adsorbed on the surface. In terms of experimental measurements, the free energy of adsorption is usually derived for the standard state (Wei and Latour 2008).

Typically, the experimentally determined binding free energy is inferred from the binding constant, via use of the expression:

$$\Delta G_{\mathrm{ads}} = -RTln(K_{\mathrm{ads}}).$$

However, inference of the free energy of adsorption, derived from experimental techniques such as quartz crystal microbalance (QCM), or surface plasmon resonance (SPR) measurements, via fitting of the raw data to the Langmuir isotherm (see Atkins and de Paula 2010, for more details), may also implicitly include contributions from peptide–peptide interactions (in the surface adsorbed state), in addition to the peptide-surface interactions under investigation. Corrections for this effect have been proposed (Wei and Latour 2008) to address this challenging problem.

2.3 Basic Key Concept: Energy Landscapes

To interpret physical chemistry observations, we need to establish links between entities such as free energy and reaction rates (in our case, e.g., rates for surface adsorption and desorption), and the structure and dynamics of the peptide, at the atomistic level. Here, we introduce and elaborate on the concept of energy landscape theory (Wales 2003; Wales et al. 1998), to reveal and interpret these links. Energy landscape theory is a unifying framework for understanding and interpreting both thermodynamic and kinetic behaviors of a system at the atomistic level. Herein, we outline the basic concepts in energy landscape theory and relate this to peptide-materials interactions.

The potential energy of a chemical system comprises the total of all inter-atomic interactions, between all atoms in the system. Typically, these potential energy contributions vary with the inter-atomic distances between all atoms in the system. Therefore, we can express the potential energy of our system as a function of the positions, e.g., in three-dimensional Cartesian space, of all atoms in this system. The position of each atom can be expressed as three scalars (numbers), e.g., corresponding to the coordinates of the atom in space (*x, y, z*). It is usual to simplify this further, and express the potential energy in terms of the number of vibrational degrees of freedom of the system. Consider a general system comprising a single, nonlinear molecule with N atoms. This system has $3N$-6 vibrational degrees of freedom (see Atkins and de Paula 2010, for more details); 3 degrees of freedom are subtracted for bulk translation along the *x, y* and *z* principal axes, and a further three are subtracted for bulk rotations around the *x, y* and *z* principal axes. This is because the potential energy captures the interactions between all atoms in the system, and the bulk translation and rotations of the system do not alter the inter-atomic distances in the system. For example, the molecule butane C_4H_{10} has 14 atoms, and thus has 36 vibrational degrees of freedom. We can therefore represent the potential energy of butane as a 36-dimensional function, and thus the potential energy surface has 37 dimensions. In order to process such a multidimensional surface, it is usual to take lower-dimensional "slices" through this surface—e.g., see Fig. 2.3 for an example of a two-dimensional slice taken from a three-dimensional potential energy surface, for a complex biomolecular system. Returning to our butane example, we can take a two-dimensional slice through the 37-dimensional surface that corresponds to the change in potential energy of butane as a function of torsion about the central carbon–carbon bond. Therefore, in general, the abscissa associated with a two-dimensional slice through a multidimensional potential energy surface corresponds to a conflation of the *3N-6* degrees of freedom, projected onto this single variable. This abscissa variable is typically referred to as a "reaction coordinate."

The key features of the potential energy surface are the stationary points—these are points on the surface where the gradient of the surface is zero. Minima on the potential energy surface are those stationary points that are convex with respect to all positions of the atoms (see Fig. 2.3). Minima on the potential energy surface

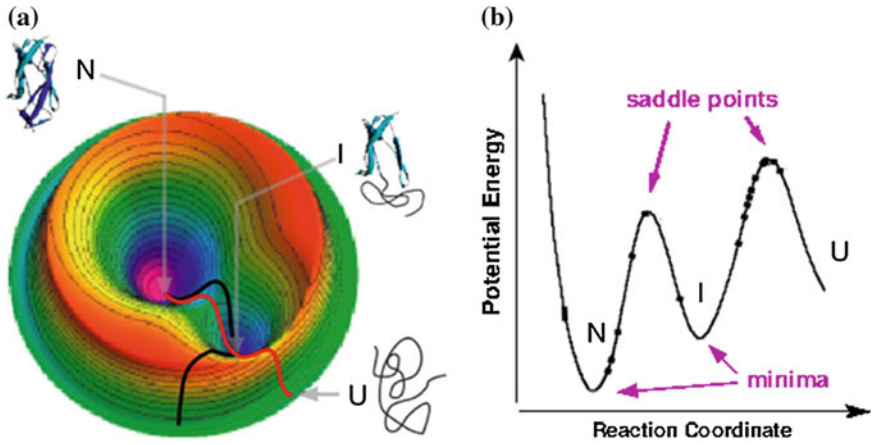

Fig. 2.3 Example of a three-dimensional potential energy surface and a two-dimensional "slice." **a** Three-dimensional surface, where stationary points *N* and *I* correspond to different stable structures. **b** The two-dimensional projection of the black pathway from the three-dimensional surface, with minima and saddle points indicated. Adapted from Schwaiger et al. (2004) EMBO reports. 6:46–51. Reproduced with permission of the copyright holder

correspond with experimentally-observable structures. The other relevant type of stationary point is the saddle point, where the potential energy is concave with respect to at least 1 degree of freedom (see Fig. 2.3). First-order saddles correspond with transition-states. Transition from one minimum to another (i.e., interconversion between two structures) can proceed via transition-states or, less directly, via higher-order saddle points (Wales 2003).

It is well-known that the number of atoms in the system is broadly connected to the number of minima supported on the potential energy surface (Wales 2003). The minimum of lowest energy on the potential energy surface is denoted the global minimum. Therefore, for a large, complex system—such as the aqueous peptide-inorganic interface—it is more likely that individual minima are many in number and comprise very small details in the overall scale of the relevant features of the potential energy surface. In this instance, collections of individual minima, grouped into *basins* (on a coarser spatial resolution) are a more appropriate level of description—and instead, we refer to the broader *potential energy landscape* (PEL).

The distribution of minima/basins in the PEL allows the prediction (or interpretation) of the equilibrium thermodynamic properties of the system. In other words, if we can determine the number of basins as a function of potential energy of these basins, as well as the shape of these basins, we can gain insight into the equilibrium properties of the system, such as the relative free energy corresponding to different configurations of the system, as a function of a (typically small) set of relevant "reaction coordinates." In the case of the aqueous peptide-inorganic interface, the distance between the peptide (say, the center of mass) and the materials surface is an appropriate reaction coordinate. The distribution of

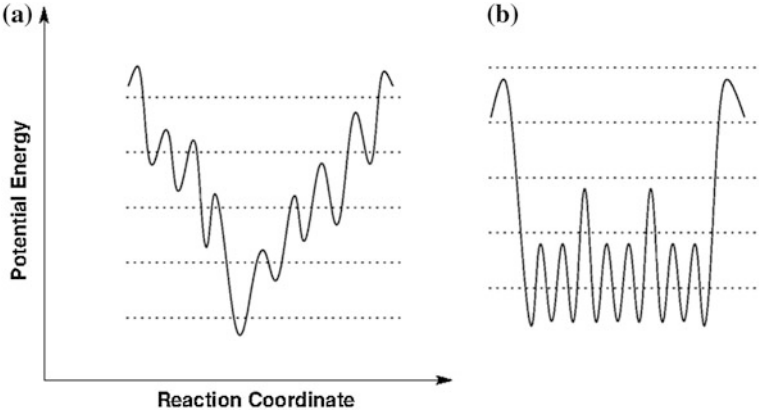

Fig. 2.4 Two exemplar potential energy landscapes projected into two dimensions. **a** Landscape corresponding to a steep funnel with moderate energy barriers between minima. **b** Landscape corresponding to a frustrated system with large barriers located between roughly iso-energetic minima. The ensemble of surface-adsorbed states for a typical materials-binding peptide could resemble example (**b**). Adapted from Wales et al. (1998). Reproduced with permission from the copyright owner

energetic barriers between basins on the PEL—in other words, the distribution of saddle points, and the minima/basins they connect, as a function of potential energy—gives us insight into the kinetics of the system. In particular, the identification of large barriers between basins can indicate basins (including those not necessarily very low in energy) that correspond with metastable configurations of the system. This information about kinetic barriers and possible metastable states is particularly important for ensuring reliable descriptions of the system using molecular simulation techniques (see Sect. 2.5). Representative, exemplar PELs, and their corresponding equilibrium and kinetic properties, are well documented (Wales et al. 2003), see Fig. 2.4. Perhaps the most well-recognized exemplar PEL is that of the protein-folding "funnel" (Bryngelson et al. 1995). On the other hand, of relevance to the aqueous peptide-materials interface is the "frustrated" or "rugged" energy landscape, characterized by large numbers of approximately iso-energetic minima/basins, separated by barriers of height much greater than k_BT (where k_B is Boltzmann's constant and T is the system temperature) (Wales et al. 1998)—see Fig. 2.4 and Sect. 2.4 for more details.

The distribution of basins/minima on the PEL, and the relative volume of these basins (in multidimensional space) can be used to roughly gauge the relative free energy of the configurations associated with these basins. Consider an example of a hypothetical PEL that features two basins: one is broad and shallow, one is narrow and deep—see Fig. 2.5. We could, for instance, relate the volume of the basin to the relative population of this basin, with respect to the total ensemble of basins, at a given temperature. Using an arbitrary energy cut-off for evaluation of the relative volume of each basin, indicated by the dashed line in Fig. 2.5. it is entirely plausible that the two basins, while having very different well-depths in

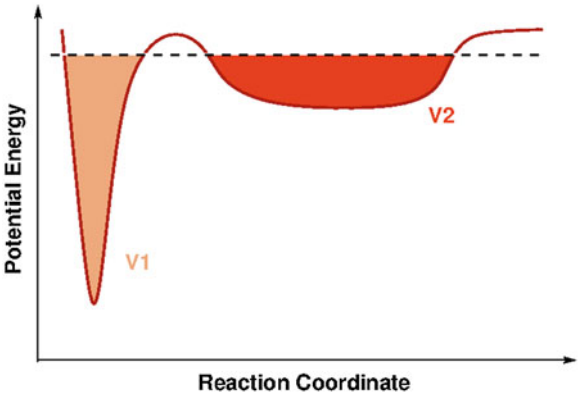

Fig. 2.5 Schematic of a hypothetical potential energy landscape projected into two dimensions. The volume of each basin, relative to a given cut-off (*black dashed line*) is indicated by the filled areas in 2-D, with the deep narrow basin corresponding with volume *V1*, and the shallow broad basin corresponding with volume *V2*

terms of potential energy, could support very similar volumes (*V1* and *V2* in Fig. 2.5), and thus, be roughly equivalent in terms of relative free energy, for that given energetic cut-off. In terms of interpreting peptide-materials adsorption, consider three hypothetical cases. In Case 1, a peptide that features a strong materials-binding affinity (i.e., a large and negative free energy of adsorption) is attributed to a multitude of relatively-weakly-bound adsorbed peptide configurations (i.e., a multitude of broad. shallow basins). In Case 2, a different peptide sequence also showing strong materials-binding affinity, is ascribed to a relatively fewer number relatively-strongly bound adsorbed peptide configurations; i.e., corresponding to a smaller number of deeper, narrow basins, where the collective volume of these narrow basins is roughly equivalent to the collective volume of the greater number of shallow basins in Case 1. Conversely, in Case 3, one could propose a peptide with a relatively weaker binding affinity, ascribed to a PEL with, say, just one single deep, narrow basin, with a volume smaller than that of the collective volumes in Cases 1 and 2. In summary, the binding affinity of a peptide is not just about the lowest-energy configuration (as illustrated by Case 3), but instead can be attributed to a combination of (1) the shape (breadth and depth) of the basins corresponding to adsorbed states, and (2) the relative numbers of each type of basin (e.g., in *very* simple terms, the number of narrow and deep basins, *vs* the number of broad and more shallow basins).

2.4 Basic Key Concept: Structure-Function Relationships at the Bio-Interface

Secondary structural motifs for peptide and proteins are defined by the positions of the backbone atoms in the peptide/protein possessing a regular pattern in space. This pattern of backbone atom positions is reflected in repetitive patterning in the values of two (of the possible three) backbone dihedral angles, ϕ and ψ (see Fig. 2.6). The third backbone dihedral angle, ω, describes the twist about the amide bond, and is thus typically considered to be rather rigid under ambient

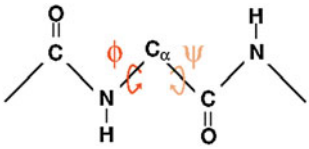

Fig. 2.6 Illustration of the two relevant dihedral angles for the peptide backbone; *phi* (defined by the C'-N-Cα-C dihedral), ϕ, and *psi* (defined by the N-Cα-C-N' dihedral), ψ

conditions. Some examples of secondary-structure classifications include α-helix, β-sheet, β-turn, and polyproline II helix (PPII). The term *random coil* does not correspond with one single secondary structure, but in its most fundamental definition, based on ideal polymer models, the Flory random coil (Flory 1969), refers to the conditions under which the backbone dihedral angles of each residue in a peptide sequence are independent of their neighbors in the sequence (Mao et al. 2013), and thus, in principle (but not usually truly in practice), should represent an ensemble of conformations where all possible conformations are sampled. On the whole, many materials-binding peptides, identified from peptide selection experiments have been found to be lacking in well-defined secondary-structure, both when free in solution and when adsorbed at the aqueous materials interface (Collino and Evans 2008; Hnilova et al. 2008; Oren et al. 2010; Slocik et al. 2011), with random coil and PPII being dominant structural assignments. In some instances, chiefly those derived from naturally occurring mineral-binding proteins (Keene et al. 2010; Delak et al. 2009), the peptide is thought to gain structural ordering upon adsorption to the target material. These structural data have led to the proposal that some materials-binding peptides could be classified as intrinsically disordered (Collino and Evans 2008).

The relationship between the well-defined three-dimensional (3-D) structure of a protein or peptide, and its function, is a paradigm that is evolving. It is now established that well-defined 3-D structure is a sufficient, but not a necessary condition for conferring function. In other words, there exist a significant number of proteins, over 40 % of the human proteome (Jensen et al. 2010), that either fully lack a well-defined folded structure, or are partially unstructured, in their *functional* form. These proteins and peptides form a class known as Intrinsically Disordered Proteins/Peptides, IDPs (Dunker et al. 2008; Tompa 2012). IDPs are thus thought to be conformationally labile; and in many (but not all) instances may show propensity to fold upon exposure to an external stimulus—such as binding to a target (Xie et al. 2007). Not only may an IDP fold upon binding to a target, the IDP also may be amenable to binding multiple targets, and the resultant conformation may also be target-dependent (Keene et al. 2010).

It is challenging to characterize the conformational heterogeneity inherent to IDP systems. This structural characterization is necessary, however, in order to construct required links between the protein/peptide sequence, the ensemble of conformations supported by this sequence, and the functionality of this sequence—namely the materials-binding affinity and/or selectivity. The techniques for this

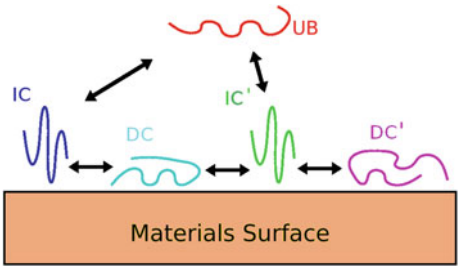

Fig. 2.7 Schematic of the proposed interconversion between various configurations in the peptide-materials interfacial system. IC and IC' denote "indirect contact" states, where the peptide may interact with the surface via a structured solvent layer. DC and DC' represent "direct contact" states where the peptide-materials interaction is not solvent mediated. UB represents the ensemble of configurations where the peptide is not bound at the materials surface

task in widespread use are nuclear magnetic resonance (NMR) spectroscopy and circular dichroism (CD) spectroscopy, although other techniques such as small angle X-ray scattering (SAXS), electron spin resonance (ESR) and fluorescence correlation spectroscopy (FCS) have also been extensively employed in the study of IDPs in general (Eliezer 2009). Given that most materials-binding peptide sequences identified from peptide selection experiments are not long (typically 7 or 12 residues), NMR, and particularly CD spectroscopy, have comprised the principal characterization tools (Collino and Evans 2008; Hnilova et al. 2008; Oren et al. 2010), and furthermore, have been applied chiefly to the characterization of the peptide structures free in solution (i.e,. not bound at the interface). There is still a good deal that is unknown regarding the archetypal structure of potential energy landscape(s) associated with IDPs in general (Fisher and Stultz 2011), and materials-binding peptides in particular.

The ensemble of peptide conformations in the presence of the aqueous materials interface is anticipated to be complex. In addition to the equilibrium partitioning of the peptide between the adsorbed and desorbed states, interconversion between different adsorbed peptide conformations may also take place (see schematic in Fig. 2.7), in addition to peptide diffusion and subsequent structural change due to peptide–peptide interactions (So et al. 2009; Nergiz et al. 2013). Therefore, gaining direct structural information of materials-binding peptides adsorbed at the materials interface, under aqueous conditions, at the atomistic level, remains a significant challenge. Despite these challenges, recent advances in NMR show promise in this area (Mirau et al. 2011).

The hypothesized interplay between a peptide sequence, the ensemble of structures that is supported by this sequence, and the binding propensity and selectivity conferred by the peptide, is pivotal to understanding, and ultimately, predicting and designing materials-binding sequences with tailored interfacial properties. Due to the challenges in obtaining direct structural data, the basis for this hypothesis has been compiled from indirect evidence from experimental sources. Compelling evidence exists regarding the impact of peptide sequence on binding

selectivity; for example, the sequence AQNPSDNNTHTH was found to bind with high affinity to GaAs, but with low affinity to silica (Goede et al. 2004). Random scrambling of this sequence to TNHDHSNAPTNQ was shown to abolish this binding selectivity, such that the sequence adsorbed to both materials with similar binding strengths (Goede et al. 2004). This finding clearly underscores the idea that the binding affinity cannot be a mere additive function of a number of strongly binding residues alone. While data such as these are helpful in developing our understanding, at present, the complex relationship between sequence, structure(s), and materials binding for these bio interfaces is still not well-defined to date. For example, for a range of materials that have been previously studied (e.g., titania, silica, gold, and so forth), there is not necessarily a clear, consensus pattern in the sequences that have identified as the strong-binding peptides, *vs* the weak binding sequences. Bioinformatics approaches are one promising route to identifying such nonobvious patterns in sequence similarity—see Sect. 2.5 for more details.

Given the experimental challenges in direct structural determination of these systems, links between peptide sequence and materials-binding affinity/selectivity can be further elucidated, in partnership with indirect experimental observations, by using computational modeling at the atomistic level. In addition, bioinformatics approaches have the potential to harness existing experimental data to identify sequence motifs with predictable binding behaviors, potentially paving the way for tailored sequence design in future.

2.5 Links to Computational Approaches

While a detailed overview of molecular simulation methods is provided in a later chapter, we conclude this introductory chapter with some brief comments relating computational approaches to both energy landscapes and structure-function relationships, in relation to the study of peptide-materials interfaces. Herein, we will briefly touch on aspects of two computational approaches; molecular simulation from the viewpoint of the potential energy landscape, and bioinformatics approaches from the viewpoint of the structure-function relationships for materials-binding peptides.

We start with a discussion of molecular simulation approaches, with particular attention on the challenge of recovering the ensemble of conformations inherent to an IDP system. The archetypal structure of potential energy landscapes (PEL) that are typical of materials binding peptide behavior have not yet been mapped out. However, for other IDP systems, initial discussions of the PEL and how this relates to the structure(s) and dynamics of these peptides and proteins is appearing in the literature (Fisher and Stultz 2011).

Because any molecular simulation approach for IDPs must be able to locate all of the relevant stable conformations (some of which may be separated by high energy barriers) and thus recover the Boltzmann-weighted ensemble of conformations, the clear need for advanced conformational sampling approaches in

modeling IDP systems is now well established (Ostermeir and Zacharias 2013). A variety of simulation strategies as applied to IDP modeling have been reported. Replica-Exchange-based approaches (Ostermeir and Zacharias 2013; Narayanan et al. 2012; Wright and Walsh 2013; Schneider and Colombi-Ciacchi 2012; Mittal et al. 2013; Knott and Best 2012; Vellore et al. 2010; Wang et al. 2008), 'divide and conquer' approaches (Sethi et al. 2012), extreme long-timescale simulation (hundreds of μsec of continuous trajectory) (Lindorff-Larsen et al. 2012), multiscale enhanced sampling (Moritsugu et al. 2012), multiscale ensemble modeling (Terakawa and Takada 2011), multicanonical MD (Higo et al. 2011). While extreme long-timescale simulations may be accessible to a fortunate few, replica-exchange-based approaches and variants thereof may provide a promising route that is more accessible to a wider range of researchers in this field. The few instances of advanced sampling approaches applied to materials binding peptides have employed replica-exchange-based approaches (Wang et al. 2008; Vellore et al. 2010; Schneider and Colombi-Ciacchi 2012; Wright and Walsh 2013). Methods development and testing of advanced sampling approaches for IDPs, including materials binding peptides, are expected to be a rapidly growing aspect of this research area, with many of the simulation studies cited here appearing in the past 1–2 years.

Another emerging computational approach that is poised for promising future growth is related to knowledge-based design and bioinformatics. In these approaches, a direct link can be made between the materials-binding propensity of a peptide sequence and the sequence itself, thus connecting nonobvious patterns in sequence to predictable binding behaviors. One such example of this approach is RosettaSurface (Masica and Gray 2009), which, for example has been used to design protein-biomineralization systems for calcite (Masica et al. 2010). In an alternative approach, a large dataset of experimental binding data for quartz-binding peptide sequences was successfully exploited to adapt common bioinformatics scoring matrices (Oren et al. 2007). This led to the prediction and verification of new silica-binding sequences with tailored binding affinity (both strong and weak), including sequences that bound stronger than the strongest binding peptide in the experimental dataset (Oren et al. 2007). Subsequent analysis of common sequence motifs (sequence dyads, triads, and tetrads) in the predicted silica-binding sequences was also compared against motifs identified from molecular simulation data, with very good agreement found between the two (Oren et al. 2010). However, the success of this approach hinged on the availability of a large set of experimentally determined binding data (Oren et al. 2007). This obstacle notwithstanding, a combination of experiment, informatics and molecular simulation could further prove to be an effective future direction for generating broader insights into sequence↔structure(s)↔binding interplay for a wide range of peptide-materials interfaces.

Acknowledgments TRW gratefully recognizes the enormously valuable contributions from members of her research group past and present, who have worked in this research field: Dr. Adam Skelton, Dr. Taining Liang, Dr. Rebecca Notman, Dr. Susana Tomasio, Simon Friling,

Louise Wright, Aaron Brown, Jasmine Desmond, Dr J. Pablo Palafox-Hernandez, Dr Zak Hughes, Kurt Drew, Anas Sultan and Andrew Church. TRW also acknowledges helpful discussions with colleagues and collaborators, from both experiment and theory, in the field of peptide-surface interactions: M. R. Knecht, R. R. Naik, R. A. Latour, J. S. Evans, S. Corni, L. Colombi-Ciacchi, S. Monti, M. Sarikaya, C. Tamerler, E. E. Oren, C. C. Perry, C. L. Freeman, P. M. Rodger, M. P. Allen, J. D. Gale, S. L. S. Stipp, J. H. Harding, M. T. Swihart and P. N. Prasad. Funding from the EPSRC, AFOSR, Deakin University and the AOARD is gratefully acknowledged. TRW thanks **veski** for an Innovation Fellowship.

References

Atkins PW, de Paula J (2010) Physical chemistry, 9th edn. OUP, Oxford

Binnig G, Rohrer H, Gerber CH, Weibel E (1983) 7 × 7 Reconstruction on Si(111) resolved in real space. Phys Rev Lett 50:120–123

Brown S (1997) Metal-recognition by repeating polypeptides. Nat Biotechnol 15:269–272

Bryngelson JD, Onuchic JN, Socci ND, Wolynes PG (1995) Funnels pathways, and the energy landscape of protein-folding—a synthesis. Proteins 21:167–195

Crookes-Goodson WJ, Slocik JM, Naik RR (2008) Bio-directed synthesis and assembly of nanomaterials. Chem Soc Rev 37:2403–2412

Chiu CY, Li Y, Huang Y (2010) Size-controlled synthesis of Pd nanocrystals using a specific multifunctional peptide. Nanoscale 2:927–930

Collino S, Evans JS (2008) Molecular specifications of a mineral modulation sequence derived from the aragonite-promoting protein n16. Biomacromolecules 9:1909–1918

Cui Y, Kim SN, Jones SE, Wissler LL, Naik RR, McAlpine MC (2010) Chemical functionalization of graphene enabled by phage displayed peptides. Nano Lett 10:4559–4565

Delak K, Harcup C, Lakshminarayanan R, Sun Z, Fan YW, Moradian-Oldak J, Evans JS (2009) The tooth enamel protein, porcine amelogenin, is an intrinsically disordered protein with an extended molecular configuration in the monomeric form. Biochemistry 48:2272–2281

Dickerson MB, Sandhage KH, Naik RR (2008a) Protein- and peptide-directed syntheses of inorganic materials. Chem Rev 108:4935–4978

Dickerson MB, Jones SJ, Cai Y, Ahmad G, Naik RR, Kroeger N, Sandhage KH (2008b) Identification and design of peptides for the rapid, high-yield formation of nanoparticulate TiO_2 from aqueous solutions at room temperature. Chem Mater 20:1578–1584

Dunker AK, Silman I, Uversky VN, Sussman JL (2008) Function and structure of inherently disordered proteins. Curr Opin Struct Biol 18:756–764

Eliezer D (2009) Biophysical characterization of intrinsically disordered proteins. Curr Opin Struct Biol 19:23–30

Estephan E, Saab MB, Martin M, Larroque C, Cuisinier FJG, Briot O, Ruffenach S, Moret M, Gergely C (2011) Phages recognizing the indium nitride semiconductor surface via their peptides. J Pept Sci 17:143–147

Fang Y, Poulsen N, Dickerson MB, Cai Y, Jones SJ, Naik RR, Kroeger N, Sandhage KH (2008) Identification of peptides capable of inducing the formation of titania but not silica via a subtractive bacteriophage display approach. J Mater Chem 18:3871–3875

Fisher CK, Stultz CM (2011) Constructing ensembles for intrinsically disordered proteins. Curr Opin Struct Biol 21:426–431

Flory PJ (1969) Statistical Mechanics of Chain Molecules. OUP, New York

Forbes LM, Goodwin AP, Cha JN (2010) Tunable size and shape control of platinum nanocrystals from a single peptide sequence. Chem Mater 24:6524–6528

Goede K, Busch P, Grundmann M (2004) Binding specificity of a peptide on semiconductor surfaces. Nano Lett 4:2115–2120

Gungormus M, Fong H, Kim IW, Evans JS, Tamerler C, Sarikaya M (2008) Regulation of in vitro calcium phosphate mineralization by combinatorially selected hydroxyapatite-binding peptides. Biomacromolecules 9:966–973

Guo J, Catchmark JM, Mohamed MNA, Benesi AJ, Tien M, Kao TH, Watts HD, Kubicki JD (2013) Identification and characterization of a cellulose binding heptapeptide revealed by phage display. Biomacromolecules 14:1795–1805

Hassenkam T, Mitchell AC, Pedersen CS, Skovbjerg LL, Bovet N, Stipp SLS (2012) The low salinity effect observed on sandstone model surfaces. Colloid Surf A 403:79–86

Heinz H, Farmer BL, Pandey RB, Slocik JM, Patnaik SS, Pachter R, Naik RR (2009) Nature of molecular interactions of peptides with gold, palladium and pd-au bimetal surfaces in aqueous solution. J Am Chem Soc 131:9704–9714

Higo J, Nishimura Y, Nakamura H (2011) A free energy landscape for coupled folding and binding of an intrinsically disordered protein in explicit solvent from detailed all-atom simulations. J Am Chem Soc 133:10448–10458

Hnilova M, Oren EE, Seker UOS, Wilson BR, Collino S, Evans JS, Tamerler C, Sarikaya M (2008) Effect of molecular conformations on the adsorption behavior of gold-binding peptides. Langmuir 24:12440–12445

Jensen MR, Salmon L, Nodet G, Blackledge M (2010) Defining conformational ensembles of intrinsically disordered and partially folded proteins directly from chemical shifts. J Am Chem Soc 132:1270–1272

Keene EC, Evans JS, Estroff LA (2010) Matrix interactions in biomineralization: aragonite nucleation by an intrinsically disordered nacre polypeptide, n16N, associated with a beta-chitin substrate. Cryst Growth Des 10:1383–1389

Knott M, Best RB (2012) A preformed binding interface in the unbound ensemble of an intrinsically disordered protein: evidence from molecular simulations. PLoS Comp Biol 8:e1002605-1-10

Kulp JL, Shiba K, Evans JS (2005) Probing the conformational features of a phage display polypeptide sequence directed against single-walled carbon nanohorn surfaces. Langmuir 21:11907–11914

Lee SW, Mao C, Flynn CE, Belcher AM (2002) Ordering of quantum dots using genetically engineered viruses. Science 296:892–895

Li CM, Botsaris GD, Kaplan DL (2002) Selective in vitro effect of peptides on calcium carbonate crystallization. Cryst Growth Des 2:387–393

Li YJ, Whyburn GB, Huang Y (2009) Specific peptide regulated synthesis of ultrasmall platinum nanocrystals. J Am Chem Soc 131:15998–15999

Lindorff-Larsen K, Trbovic N, Maragakis P, Piana S, Shaw DE (2012) Structure and dynamics of an unfolded protein examined by molecular dynamics simulation. J Am Chem Soc 134:3787–3791

Mao AH, Lyle N, Pappu RV (2013) Describing sequence-ensemble relationships for intrinsically disorderd proteins. Biochem J 449:307–318

Masica DL, Gray JJ (2009) Solution- and adsorbed-state structural ensembles predicted for the statherin-hydroxyapatite system. Biophys J 96:3082–3091

Masica DL, Schrier SB, Specht EA, Gray JJ (2010) De novo design of peptide-calcite biomineralization systems. J Am Chem Soc 132:12252–12262

Mirau PA, Naik RR, Gehring P (2011) Structure of peptides on metal oxide surfaces probed by NMR. J Am Chem Soc 133:18243–18248

Mittal J, Yoo TH, Georgiou G, Truskett TM (2013) Structural ensemble of an intrinsically disordered peptide. J Phys Chem B 117:118–124

Moritsugu K, Terada T, Kidera A (2012) Disorder-to-order transition of an intrinsically disordered region of sortase revealed by multiscale enhanced sampling. J Am Chem Soc 134:7094–7101

Naik RR, Brott L, Carlson SJ, Stone MO (2002a) Silica precipitating peptides isolated from a combinatorial phage display library. J Nanosci Nanotechnol 2:95–100

Naik RR, Stringer SJ, Agarwal G, Jones SE, Stone MO (2002b) Biomimetic synthesis and patterning of silver nanoparticles. Nat Mater 1:169–172

Narayanan C, Weinstock DS, Wu KP, Baum J, Levy RM (2012) Investigation of the polymeric properties of α-synuclein and comparison with NMR experiments: a replica exchange molecular dynamics study. J Chem Theory Comput 8:3929–3942

Nergiz SZ, Slocik JM, Naik RR, Singamaneni S (2013) Phys Chem Chem Phys 15:11629–11633

Nygaard S, Wendelbo R, Brown S (2002) Surface-specific zeolite-binding proteins. Adv Mater 14:1853–1856

Oren EE, Tamerler C, Sahin D, Hnilova M, Seker UOS, Sarikaya M, Samudrala R (2007) A novel knowledge-based approach to design inorganic binding peptides. Bioinformatics 23:2816–2822

Oren EE, Notman R, Kim IW, Evans JS, Walsh TR, Samudrala R, Tamerler C, Sarikaya M (2010) Probing the molecular mechanisms of quartz-binding peptides. Langmuir 26:11003–11009

Ostermeir K, Zacharias M (2013) Advanced replica-exchange sampling to study the flexibility and plasticity of peptides and proteins. Biochim Biophys Acta 1834:847–853

Patwardhan SV, Emami FS, Berry RJ, Jones SE, Naik RR, Deschaume O, Heinz H, Perry CC (2012) Chemistry of aqueous silica nanoparticle surfaces and the mechanism of selective peptide adsorption. J Am Chem Soc 134:6244–6246

Pender MJ, Sowards LA, Hartgerink JD, Stone MO, Naik RR (2006) Peptide-mediated formation of single-wall carbon nanotube composites. Nano Lett 6:40–44

Pilling MJ, Seakins PW (2001) Reaction kinetics. OUP, Oxford

Puddu V, Perry CC (2012) Peptide adsorption on silica nanoparticles: evidence of hydrophobic interactions. ACS Nano 6:6356–6363

Rothenstein D, Claasen B, Omiecienski B, Lammel P, Bill J (2012) Isolation of ZnO-Binding 12-mer peptides and determination of their binding epitopes by NMR spectroscopy. J Am Chem Soc 134:12547–12556

Roy MD, Stanley SK, Amis EJ, Becker ML (2008) Identification of a highly specific hydroxyapatite-binding peptide using phage display. Adv Mater 20:1830–1836

Ruan LY, Ramezani-Dakhel H, Chiu CY, Zhu E, Li YJ, Heinz H, Huang Y (2013) Tailoring molecular specificity toward a crystal facet: a lesson from biorecognition toward Pt{111}. Nano Lett 13:840–846

Sano KI, Shiba K (2003) A hexapeptide motif that electrostatically binds to the surface of titanium. J Am Chem Soc 125:14234–14235

Sarikaya M, Tamerler C, Jen A-K, Schulten K, Baneyx F (2003) Molecular biomimetics: nanotechnology through biology. Nat Mater 2:577–585

Sarikaya M, Tamerler C, Schwartz DT, Baneyx F (2004) Materials assembly and formation using engineered polypeptides. Annu Rev Mater Res 34:373–408

Schneider J, Colombi Ciacchi L (2012) Specific material recognition by small peptides mediated by the interfacial solvent structure. J Am Chem Soc 134:2407–2413

Serizawa T, Techawanitchai P, Matsuno H (2007) Isolation of peptides that can recognize syndiotactic polystyrene. ChemBioChem 8:989–993

Sethi A, Tian J, Vu DM, Gnanakaran S (2012) Identification of minimally interacting modules in an intrinsically disordered protein. Biophys J 103:748–757

Skelton AA, Liang TN, Walsh TR (2009) Interplay of sequence, conformation, and binding at the peptide-titania interface as mediated by water. ACS Appl Mater Interfaces 1:1482–1491

Slocik JM, Govorov AO, Naik RR (2011) Plasmonic circular dichroism of peptide-functionalized gold nanoparticles. Nano Lett 11:701–705

So CR, Kulp JL, Oren EE, Zareie H, Tamerler C, Evans JS, Sarikaya M (2009) Molecular recognition and supramolecular self-assembly of a genetically engineered gold binding peptide on Au{111}. ACS Nano 3:1525–1531

Tamerler C, Duman M, Oren EE, Gungormus M, Xiong X, Kacar T, Parviz BA, Sarikaya M (2006) Materials specificity and directed assembly of a gold-binding peptide. Small 2:1372–1378

Terakawa T, Takada S (2011) Multiscale ensemble modelling of intrinsically disordered proteins: p53 N-terminal domain. Biophys J 101:1450–1458

Thai CK, Dai H, Sastry MSR, Sarikaya M, Schwartz DT, Baneyx F (2004) Identification and characterization of Cu_2O- and ZnO-binding polypeptides by Escherichia coli cell surface display. J Biotech Bioeng 87:129–137

Tompa P (2012) Intrinsically disordered proteins: a 10-year recap. Trends Biochem Sci 37:509–516

Vellore NA, Yancey JA, Collier G, Latour RA, Stuart SJ (2010) Assessment of the transferability of a protein force field for the simulation of peptide-surface interactions. Langmuir 26:7396–7404

Wales DJ (2003) Energy landscapes. CUP, Cambridge

Wales DJ, Miller MA, Walsh TR (1998) Archetypal energy landscapes. Nature 394:758–760

Wang SQ, Humphreys ES, Chung SY, Delduco DF, Lustig SR, Wang H, Parker KN, Rizzo NW, Subramoney S, Chiang YM, Jagota A (2003) Peptides with selective affinity for carbon nanotubes. Nat Mater 2:196–200

Wang F, Stuart SJ, Latour RA (2008) Calculation of adsorption free energy for solute-surface interactions using biased replica-exchange molecular dynamics. Biointerphases 3:9–18

Wei Y, Latour RA (2008) Determination of the adsorption free energy for peptide-surface interactions by SPR spectroscopy. Langmuir 24:6721–6729

Whaley SR, English DS, Hu EL, Barbara PF, Belcher AM (2000) Selection of peptides with semiconductor binding specificity for directed nanocrystal assembly. Nature 405:665–668

Whitford D (2005) Proteins: structure and function. Wiley, Chichester

Wright LB, Walsh TR (2012) Facet selectivity of binding on quartz surfaces: free energy calculations of amino-acid analogue adsorption. J Phys Chem C 116:2933–2945

Wright LB, Walsh TR (2013) Efficient conformational sampling of peptides adsorbed onto inorganic surfaces: insights from a quartz binding peptide. Phys Chem Chem Phys 15:4715–4726

Xie HB, Vucetic S, Iakoucheva LM, Oldfield CJ, Dunker AK, Uversky VN, Obradovic Z (2007) Functional anthology of intrinsic disorder. 1. Biological processes and functions of proteins with long disordered regions. J Proteome Res 6:1882–1898

http://www.springer.com/978-1-4614-9445-4

Bio-Inspired Nanotechnology
From Surface Analysis to Applications
Knecht, M.R.; Walsh, T.R. (Eds.)
2014, VIII, 314 p. 172 illus., 108 illus. in color.,
Hardcover
ISBN: 978-1-4614-9445-4